Journal of Membrane Science and Research 6 (2020) 196-202

Journal of Membrane Science & Research

journal homepage: www.msrjournal.com

Research Paper

A Facile Approach of Thin Film Coating Consisted of Hydrophobic Titanium Dioxide over Polypropylene Membrane for Membrane Distillation

Rajesha Kumar *, Mansour Ahmed, Garudachari Bhadrachari, Abbas Al-Mesri, Jibu P. Thomas

Water Research Center, Kuwait Institute for Scientific Research, P.O. Box 24885, 13109 Safat, Kuwait

Article info

Received 2019-07-07
Revised 2019-08-25
Accepted 2019-09-01
Available online 2019-09-01

Keywords

Surface coating
Hydrophobic nanoparticle
Membrane distillation
Self-assembly
Morphology

Highlights

- A hydrophobic layer was coated over the PP membrane by self-assembly of trimesic acid molecules containing phosphonic acid functionalized TiO_2 nanoparticles
- The coated membranes were porous and slightly rougher than the uncoated membrane
- The compatibility of modified TiO_2 increased by interaction with the trimesic acid molecules
- The flux, rejection, and durability of the coated membranes was much higher during seawater desalination using membrane distillation

Graphical abstract

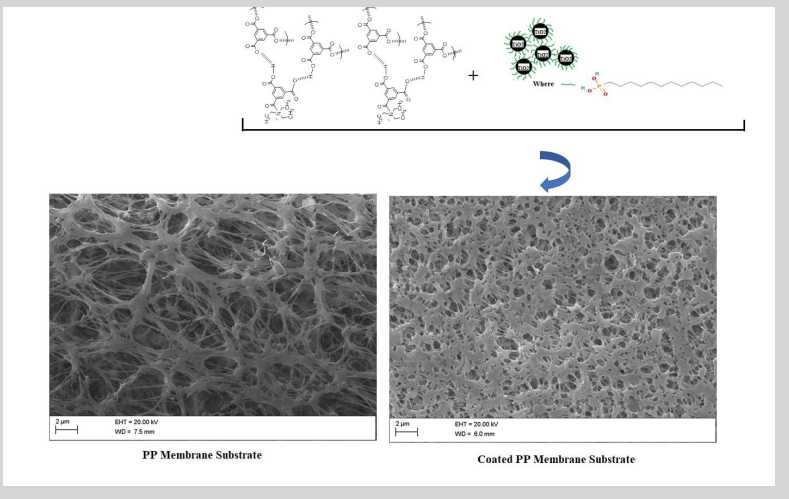

Abstract

In this work, the hydrophobic modification of TiO_2 nanoparticles ($HTiO_2$) was carried out by reacting with dodecylphosphonic acid (DDPA) and hexylamine solution. A facile approach of the self-assembly technique was used for the coating of hydrophobic $HTiO_2$ layer over the microporous polypropylene (PP) membrane. The self-assembled layer was formed between the interface of trimesoyl chloride (TMC) (in hexane) and trimethylamine (in water) solutions. The high porosity for the coated membranes ascribed to the self-assembled trimesic acid (TMA) layer and its potential to generate open and loosely packed, two-dimensional hydrogen-bond networks on the membrane surface. The dispersion of $HTiO_2$ was accomplished in the TMC in hexane leading hydrophobic and porous surfaces than the neat PP membrane. The initial average pore size of the PP membrane was reduced from 0.4 µm to 0.2 µm with a coating of 2.0 wt% of $HTiO_2$. The new membranes showed high reliability, high rejection, and water flux during the real seawater desalination tested in direct contact membrane distillation (DCMD) configuration. The maximum transmembrane permeate flux of 45.4 kg/m^{2}h with >98% salt rejection was obtained for the coating layer with 2.0 wt% $HTiO_2$ at 80ºC demonstrating the future potential application towards seawater desalination.

1. Introduction

Membrane Distillation (MD) is a thermally driven membrane-based separation process. One of the promising applications of this process is seawater desalination due to low operating temperatures than conventional process since in the MD method the water isn't essentially heat up to the boiling [1]. The working principle of MD involves vapor transport through the pores of the microporous membrane driven by the vapor pressure gradient across the membrane. The membrane characteristics resemble microfiltration membranes; however, more hydrophobic surfaces and porous structures are desired to overcome wetting and low flux issues respectively. The determination of physical characteristics such as porosity, morphology, pore size, hydrophobicity and liquid entry pressure (LEP) will help to identify the suitable membrane for the practical applications [2]. LEP is the minimum pressure at which the water starts flowing through the membrane pore. For an ideal MD membrane, LEP value should be high to avoid the membrane wetting during the MD operations. The fabrication of potential MD membranes is in a developmental stage and the researchers are focusing on

* Corresponding author: ralambi@kisr.edu.kw (R. Kumar)

DOI: 10.22079/JMSR.2019.110904.1273

the composites of hydrophobic polymers with the nanofillers for the enhanced stability and improved performance [3-5]. Polypropylene (PP) as a membrane material for MD applications offers hydrophobic surfaces owing to its high surface tension, temperature stability, less conductivity of heat, and low surface energy [1].

Despite the essential features of PP membranes towards the MD application, further modification is essential to attain high anti-wetting and antifouling characteristics during the MD application [6]. The hydrophobic modification of PP membrane can be effectively performed by coating method [7,8]. Himma et al. prepared coated PP membrane by dip-coating method to attain the superhydrophobic surface [9]. The polymer solution concentration and drying temperature have influenced the hydrophobicity. The membrane surface roughness and contact angle were increased using methyl ethyl ketone as nonsolvent. Zhou et al. used a converted PP membrane superhydrophobic PP surfaces by coating with 500-mesh PTFE-coated sieve [10]. Roy et al. used acid functionalized carbon nanotube on the PP substrate to enhance the water vapor transport through the membrane [11]. The functionalized CNT improved the flux, salt rejection and thermal stability of modified PP membrane. Xu et al. coated the PP membrane with the silica dispersed in PP solution followed by treatment with 1H,1H,2H,2H-perfluorooctyltriethoxysilane (POTS) [12] for MD application. Shao et al. achieved the fluorination of SiO_2 nanoparticles on the PP membrane to improve the roughness, hydrophobicity, and durability of the resultant MD membrane [13].

Generally, TiO_2 nanoparticles are hydrophilic and a few studies have been reported on hydrophobic surface tailoring using TiO_2. Sun et al. converted polyethersulphone membrane surface to a superhydrophobic surface by the combined reactions of silica sol treatment and fluoroalkyl silanization [14]. The modified membrane displayed a higher contact angle of 154º compared to 75º for the neat PES membrane. Guosheng et al. converted hydrophilic TiO_2 nanoparticle to hydrophobic by reacting with the silane coupling agent [15]. The wetting studies revealed that the hydrophobicity of silane- modified TiO_2 nanoparticles was increased. Amir et al. used hydrothermal method first to deposit TiO_2 and then to fluorosilanize using 1H, 1H, 2H, 2H-perfluoro-dodecyl trichlorosilane on PVDF membrane [16]. The modified membranes were superhydrophobic with a contact angle 166º and LEP value was increased to 190 kPa from 120 kPa compared to neat PP membrane. The altered PVDF membranes showed superior MD flux and higher antifouling properties. Organic phosphorous acids such as phosphonic acids and their ester derivatives are widely used to functionalize the nano-metal oxide surfaces [17]. The alkyl chains terminating with the phosphonic acid group can easily react with the active -OH groups of TiO_2 through covalent bonding [18,19]. Further, the stability of TiO_2 nanoparticles will be increased by phosphonate groups when paired with an electronegative terminating group [20,21]. The phosphonic acid modification of TiO_2 attached with long-chain alkyl groups imparts hydrophobic modification on the particle surface [22]. In this study, the first time we report the molecular self-assembly approach for the coating of hydrophobic nanoparticles on the PP membrane support. The hydrophobically modified phosphonic acid-TiO_2 nanoparticles ($HTiO_2$) are used as a nanofiller during coating over the PP membrane. Phosphonic acid groups are ideal to produce self-assembled monolayer due to the low acid dissociation constant [23,24]. The proposed approach of self-assembly is a simple interfacial reaction to generate a charged thin layer on the PP substrate. The seawater desalination of newly fabricated PP nanocomposite membranes was tested in DCMD configuration. The MD performance results are correlated with the physical and chemical characteristics of the modified PP membranes.

2. Experimental

2.1. Materials

n-Dodecylphosphonic acid (DDPA) and hexylamine were procured from Sigma Aldrich Co. Polypropylene was procured from the Petrochemical Industries Company, Kuwait. Methanol and ethyl acetate were purchased from Merck Co. TiO_2 nanoparticles dry powder anatase phase (average size of 4-8 nm) was procured from PlasmaChem GmbH. Trimesoyl chloride (TMC) and Triethylamine were acquired from Alfa Aesar Co. and Sigma Aldrich Co respectively.

2.2. Synthesis of $HTiO_2$

The chemical functionalization of TiO_2 nanoparticles involved a literature reported protocol with minor modification [25]. TiO_2 nanoparticles (0.5 g) was directly added to an excess amount of DDPA (10 mL) and the slurry was stirred at 25-26 °C for 24 h. The solids were separated from the turbid suspension by centrifugation at 4000 rpm. The excess DPPA was removed by washing with ethyl acetate (25 mL) and then by adding methanol (20 ml). The solid TiO_2 was added to additional methanol (25 mL) and reacted with the hexylamine (10 mL) by stirring for 1 h. The precipitated solids were separated by centrifugation at 4000 rpm and the excess DDPA was removed by washing with ethyl acetate (3 x 25 mL). The washed solids were dried at 60 °C before further characterization.

2.3. Preparation of PP membrane

The preparation of flat sheet PP membranes includes a melt extrusion method due to the insolubility of PP in polar organic solvents. Briefly, PP was dry blended and added into a hopper of the Twin-screw extruder instrument. The extrusion conditions include; barrel temperature: 230 °C, die temperature: 200 °C and a screw speed: 200 rpm. The precursor films were prepared by compelling molten PP polymer through a shaped film die. Finally, the precursor films were dipped in water coagulation medium. Further improvement in the porosity of the PP membranes, was achieved by the uniaxial stretching at 140 °C. The annealing and stretching of the precursor films for the improved porosity was achieved using a previously reported protocol [26].

2.4. Preparation of coated PP membranes

The membrane fabrication step involved an approach of self-assembly techniques by the coating of the nanocomposite layer over the microporous PP membrane [27]. The coating layer thickness was limited to 100 nm using a composition of 0.1 wt% TEA (in water) with 0.05 wt% of TMC (in n-Hexane). In a typical procedure, the PP membrane surface was treated with 50 mL of TEA solution for 2 min at 25 ºC to diffuse TEA molecules into pores of the PP substrate. The excess amine solution was removed by applying a compressed air gun. Now, the solution of TMC (50 mL) dispersed with $HTiO_2$ was poured on the PP membrane surface consisting of TEA. The TMC could react with TEA molecules for 2 min at 25 ºC and the unreacted TMC was removed by applying the compressed air again. The resultant membrane was cured 90 ºC for 5 min to convert TMC to trimesic acid. The hot membrane was cooled to ambient temperature and washed with deionized (DI) water and dried at 25-26 ºC. The different membranes synthesized with the membrane codes in accordance with the $HTiO_2$ composition are presented in Table 1.

Table 1
The different compositions of the synthesized PP membranes.

Membrane Code	TMC (wt%)	TEA (wt%)	$HTiO_2$ (wt%)
M-0	0.05	0.1	0.0
M-0.5	0.05	0.1	0.5
M-1.0	0.05	0.1	1.0
M-2.0	0.05	0.1	2.0
M-3.0	0.05	0.1	3.0

2.5. Membrane characterization

The Fourier Transform Infrared Spectroscopy (FTIR) spectrum of $HTiO_2$ was recorded using Attenuated total reflectance- infrared (ATR-IR) instrument from Bruker Co. (ALPHA model). The scanning electron microscope (SEM) from Zeiss was used to determine the membrane surface images and to characterize $HTiO_2$ particles. The same instrument was used to determine the pore size of the top surface of the membranes assuming that the surface pores were circular [28,29]. The pore size reported in the current study is an average pore size of 50 randomly selected pores from each membrane sample. The contact angle goniometer from USA KINO (model-SL200KB) was used to measure the surface contact angle values of membranes using the sessile drop method. The atomic force measurement (AFM) instrument from Concept Scientific Instrument (Nano-Observer), France, was used to measure the surface roughness values of membranes in resonance mode. A dead-end filtration cell purchased from Sterlitech Corporation, USA was used to evaluate the liquid entry pressure (LEP_w) values of membranes. In a typical protocol, the pressure of the feed side was increased at 0.05 MPa at each interval of 10 min and the pressure

corresponding to the first drop of water in the permeate was considered as a LEP_w point. The porosity measurement includes a gravimetric method where the membrane sample was soaked in anhydrous isopropanol for 24 h and the initial weight of the wet membrane was recorded as m_1 [30]. Then, the wetted sample was dried at 50 °C for 24 h before recording the dry weight of the membrane as m_2. The overall porosity was calculated using the following equation (1).

$$\varepsilon = \frac{(m_1 - m_2)/\rho_w}{(m_1 - m_2)/\rho_w + m_2/\rho_p} \quad (1)$$

where m_1 and m_2 are the weights of the wet and dry membranes respectively, ρ_w is the density of isopropanol (786 kg/m^3) and ρ_p is the density of the polymer (946 kg/m^3).

2.6. Flux and DCMD experimental protocol

For MD performance of the PP and coated PP membranes were tested in a custom-made multiconfiguration MD test unit from Convergence Instruments. The details of the experimental set-up and the experimentation protocol were presented in our previously reported article [31]. Briefly, the flat-sheet membrane 50 mm (diameter) was tightly clamped between the two chambers of the membrane module. The hot feed of real seawater collected from beach well of a desalination plant at Doha, Kuwait. The temperature-dependent flux study was conducted over a feed temperature range of 50-80 °C by maintaining a constant permeate (DI water) temperature at 20 °C. The flux J (kg/m^{2}h) was measured using the following equation 2.

$$J = \frac{\Delta W}{A\Delta t} \quad (2)$$

where ΔW is the weight of distillate (kg), A is the effective membrane area (m^2) and Δt is the sampling time (h). The details of the analysis of the water parameters using various instrumentation are presented in our previous article [31].

3. Results and Discussion

3.1. FTIR analysis

The FT-IR spectrum of TiO_2 nanoparticles showed different characteristic peaks as shown in Figure 1(a). In this spectrum, the broad absorption band from 3200 to 3400 cm^{-1} is attributed to stretching and 1635 cm^{-1} to bending vibration of O-H, corresponding to the moisture [32]. Compared to the TiO_2 spectrum, the $HTiO_2$ particles modified by chemically reacting with DDPA and hexylamine showed distinct characteristic peaks as shown in Figure 1(b). The chemical structure of DDPA is presented in Figure 2. In the FTIR spectrum of $HTiO_2$, the peaks corresponding to -CH_2 vibrational mode of DDPA molecules appeared at 2917 cm^{-1}, 2848 cm,$^{-1}$ and 1529 cm.$^{-1}$ The peaks at 1458 cm^{-1} and 1003 cm^{-1} corresponds to -P=O and -P-O stretching respectively [33] confirmed the DDPA modification of the TiO_2 nanoparticles.

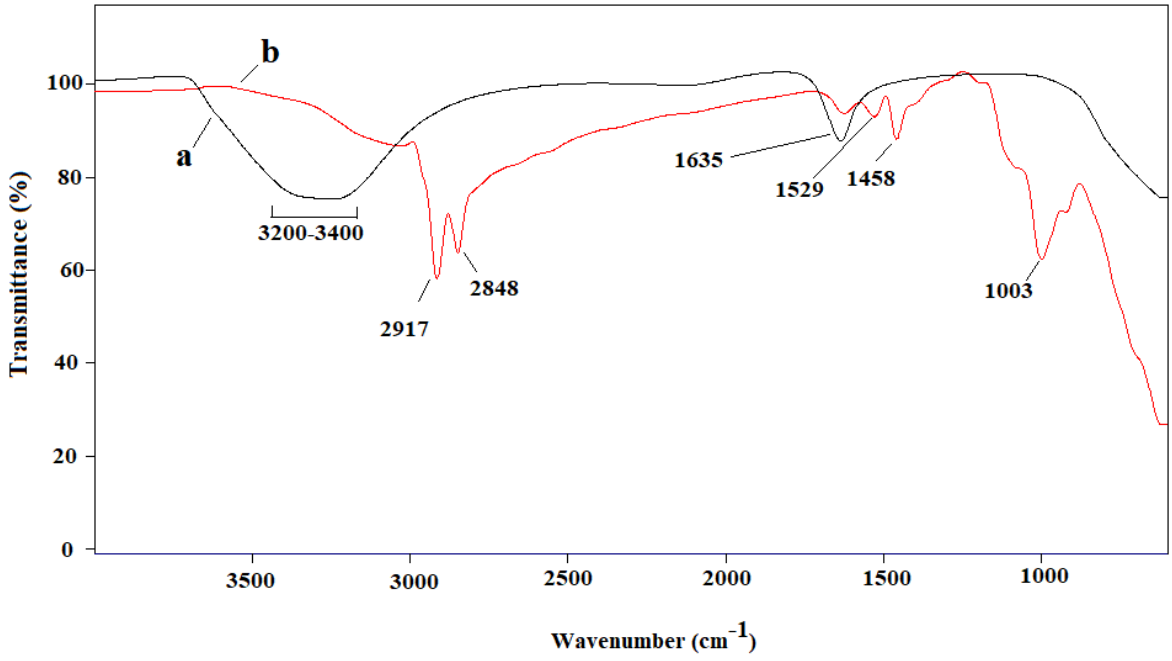

Fig. 1. FTIR spectra of a) TiO_2 nanoparticles and b) $HTiO_2$.

3.2. SEM analysis

The SEM image of $HTiO_2$ particles is presented in Figure 3. It revealed that the size of the DDPA modified particles increased between 60-180 nm attributed to the large size of DDPA chemically attached by the TiO_2 particles. The SEM analysis of the neat PP and coated PP membranes in Figure 4 revealed a drop in the pore size for the later membrane surface. The self-assembled layer penetrated in some large pores of PP support membrane by the capillary forces, providing more stability for the self-assembled layer [34]. Also, it is observed that the self-assembled TMC layer has aided the $HTiO_2$ molecules to attach firmly to the membrane surface. The homogeneous dispersion of $HTiO_2$ on the membrane without any agglomeration is attributed to TMC as a suitable solvent selected for nanoparticle dispersion. The aggregation of nanoparticles is a commonly observed phenomenon during the fabrication of nanocomposite membranes as the nanoparticles tend to reduce their high surface energy at higher concentration. The surface SEM images of M-1.0 and M-2.0 membranes quite similar, however, at an elevated loading concentration of 3.0 wt% of $HTiO_2$, the membrane surface witnessed the agglomeration of nanoparticles on the membrane surface as highlighted in Figure 4 (d). The $HTiO_2$ in the coating layer produced porous structures on the membrane surfaces as the self-assembly of TMA on a membrane substrate has a high tendency to produce open and loosely packed, two-dimensional hydrogen-bond networks at the interface [35]. The formation of porous structures is well supported in the literature as Ye et al. observed the self-

assembly of TMA on gold particles with the formation of porous flower type self-assembly structures [36]. The same study revealed the formation of porous structures of trimesic acid stabilized by hydrogen bonding.

3.3. Contact angle, pore size, porosity and liquid entry pressure,

The coated PP membranes showed higher contact angle values than the neat PP membrane as presented in Table 2. This indicated that the coated PP membranes were more hydrophobic than the nascent PP membrane. The surface modification of TiO_2 nanoparticles with DDPA has produced hydrophobic groups terminating with the phosphonic acid. The improved hydrophobicity of the coated membranes attributed to the surface modification with long-chain aliphatic groups ensuring a better dispersion in the self-assembled layer via the interfacial interactions between NPs and the matrix [37]. The introduction of long aliphatic chains on the membrane surface played a positive role in the hydrophobicity enhancement by decreasing the membrane surface free energy [31]. The average pore size of the PP membrane decreased after coating from 0.40 µm to 0.18µm for M-3.0 membrane (Table 2). The decreased pore size values for coated PP membranes complies with the ideal pore size of MD operations, which ranges between 0.1-1.0 µm [38]. The decrease in pore size is due to the partial filling of the surface pores of the PP membrane by the porous structures of the self-assembled TMC layer comprised of $HTiO_2$. The pore size reduction was proportional to the higher loading of $HTiO_2$ as revealed in Table 2. This could be the effect of increased concentration of $HTiO_2$ leading to the formation of compact self-assembled structures with reduced pore size. From Table 2, the overall porosity of coated nanocomposite PP membranes quite improved compared to the pristine PP membrane. The increase in porosity of the membrane attributed to the formation of self-assembled TMA structures on the membrane surface [36]. The nascent PP membranes showed an LEP value of 98 kPa, while for the M-2.0 membrane its value was increased to 215 kPa (Table 2). The higher value of LEPw for coated PP membranes as revealed from Table 2 indicated the increased transmembrane pressure across the membrane due to the reduced pore size after the surface coating [1,39,40].

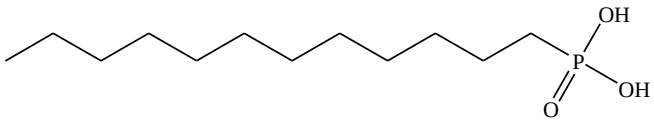

Fig. 2. Chemical structure of dodecylphosphonic acid.

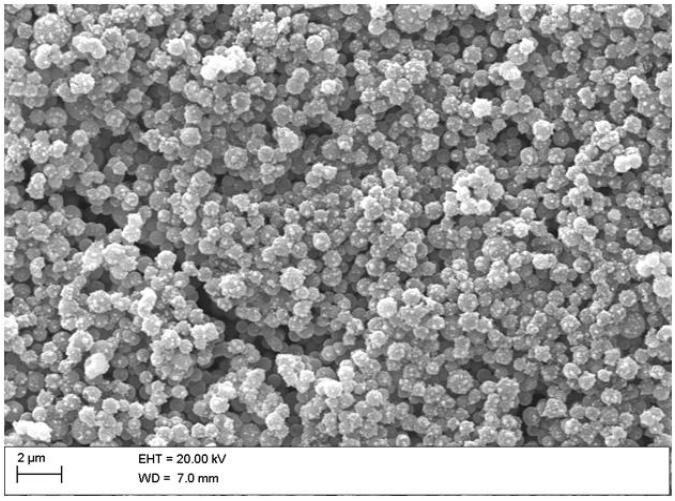

Fig. 3. SEM image of the $HTiO_2$ nanoparticles.

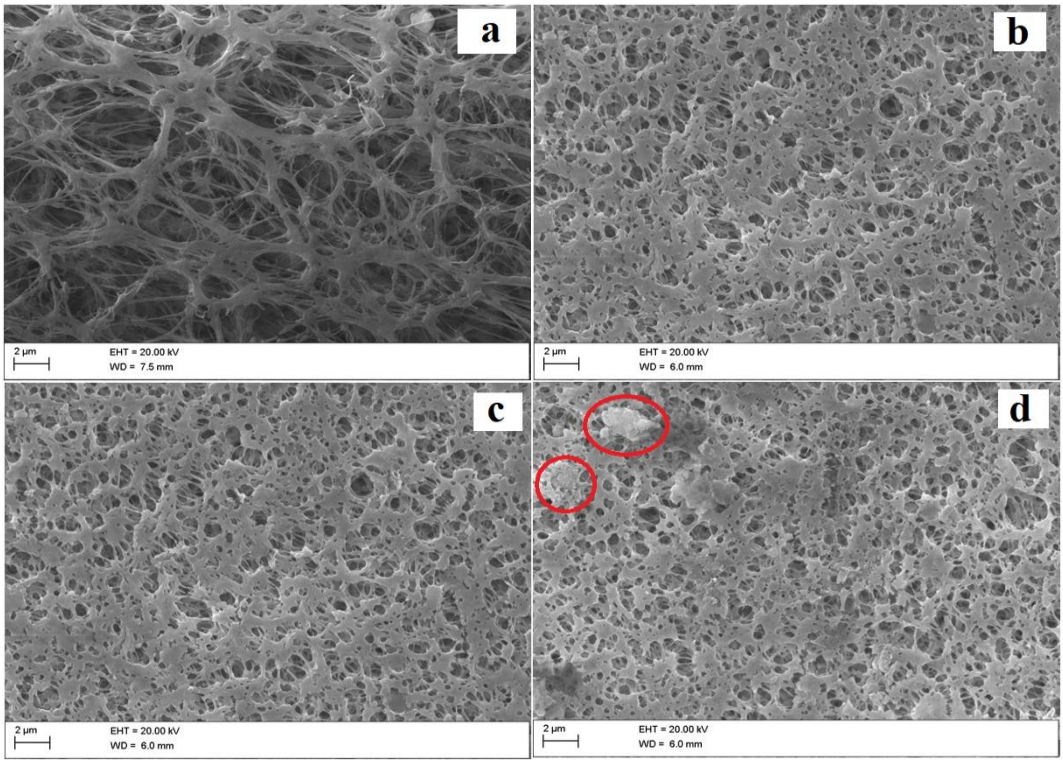

Fig. 4. Surface SEM images of a) M-0, b) M-1.0, c) M-2.0 and d) M-3.0 membranes.

3.4. AFM analysis

The 3D AFM images of the pristine PP and coated composite PP membranes at a scan size of 10 μm × 10 μm are presented in Figure 5. The AFM images revealed a slight increase in the surface roughness value for the coated PP membranes. The $HTiO_2$ modified by DDPA containing long-chain hydrophobic organic groups tend to aggregate in aqueous medium via Van der Waals interactions with the membrane surface groups [41]. In contrary, a slight increase in the average surface roughness for modified PP membrane attributed to the least aggregation of $HTiO_2$ up to the loading of 2.0 wt% due to the presence of TMC molecules in the solvent selected for the dispersion. The hydrogen-bonding interactions between the phosphonic acid groups of $HTiO_2$ and acid groups of trimesic acid molecules could be the reason for least aggregation of $HTiO_2$ for attaining control over the increased surface roughness values for the coated membranes. Generally, modifying the nanoparticle surface changes both the nanoparticle-polymer interactions and nanoparticle-nanoparticle interactions. Also, the cross-linking interactions on the membrane surface through bonding or ionic interactions reduces the surface roughness [42, 43]. Thus, the interaction of $HTiO_2$ terminating with the phosphonic acid with the self-assembled trimesic acid groups via intermolecular hydrogen bonding could be the other reason for the small increase in roughness values for the coated PP membranes.

Table 2
The physical properties of the membranes.

Membrane Code	Contact angle (°)	LEPw (kPa)	Porosity (%)	Pore size (μm)	Average surface roughness (nm)
M-0	86.6±1.1	98±3.0	55.6±0.80	0.40±0.05	100
M-0.5	90.6±2.3	146±2.0	56.1±0.63	0.35±0.02	105
M-1.0	100.3±1.9	188±4.0	57.3±0.91	0.32±0.01	112
M-2.0	110.4±2.1	215±1.0	58.1±0.43	0.20±0.03	118
M-3.0	115.5±1.8	235±2.0	57.6±0.64	0.18±0.01	122

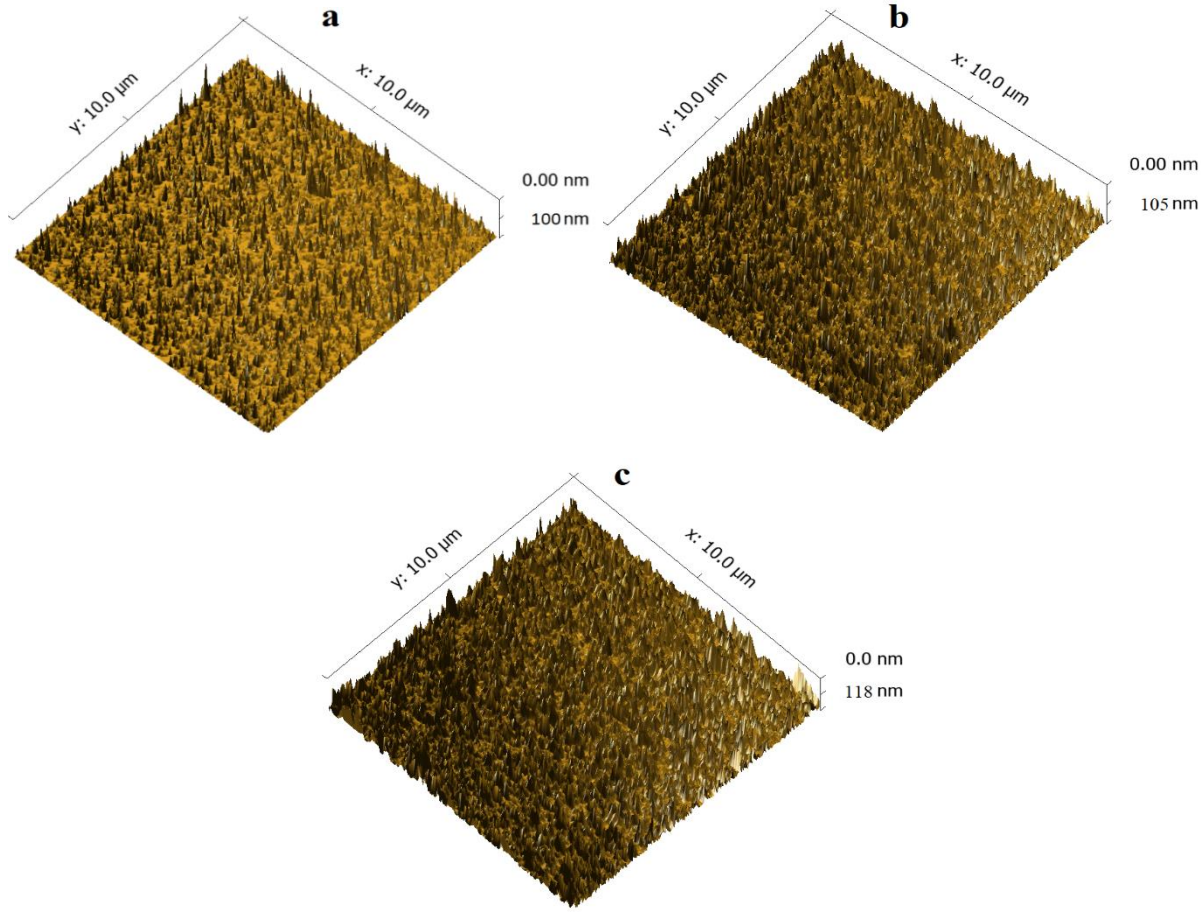

Fig. 5. The 3D-AFM images of a) M-0, b) M-0.5, and c) M-2.0 membranes.

3.5. The membrane permeation flux and seawater desalination performance

As presented in Figure 6, the permeate flux of all the coated PP membranes was much higher than the nascent PP membrane. Generally, pore size reduction has an adverse effect on the flux, but the increased porosity of the coated PP membranes had dominated effect in determining the membrane flux compared to decreased pore size. The water flux of all the membranes, increased with the increase in temperature due to the increased vapor pressure of seawater as a main driving force of the MD process [1]. In the MD process, the seawater contacted directly to the surface of neat PP membrane causing wetting of the pores. The trapped seawater can reduce the effective liquid evaporation area and causes flux reduction. However, incorporation of $HTiO_2$ into the PP membrane matrix tends to improve both the pore-wetting resistance and the evaporation area eventually increasing the membrane flux [44-46]. The increased loading of $HTiO_2$ increased the water flux as the more hydrophobic surfaces formed for the easy transport of water vapors without wetting. The rejection towards the seawater TDS for both the nascent PP and modified PP membranes was >98%. However, modified PP membranes

attained slightly improved seawater ionic rejection as presented in Table 2. From Table 2, the porosity of M-1 and M-3 were almost similar with significantly higher pore size for the M-1 membrane. However, the permeate flux of M-3 was higher than M-1, particularly at high feed temperature. The increased hydrophobicity due to the higher loading $HTiO_2$ has dominated effect on increasing the permeate flux than the reduced pore size of the membrane. The presence of hydrophobic $HTiO_2$ in the coating layer tends to reduce the membrane pore-wetting. Also, the loading of $HTiO_2$ increased the membrane total vapor evaporation area to increase the mass transfer coefficient, thereby increasing the water flux as reported in other works [47-49]. The coated PP membrane with 2.0 wt% of $HTiO_2$ corresponds to an optimum loading composition with a maximum permeate flux of 45.4 kg/m^{2}h at 80 ºC. M-3.0 membrane with higher loading of 3.0 wt % of $HTiO_2$ experienced a drop-in flux value to 43.8 kg/m^{2}h at 80 ºC due to the excess loading of $HTiO_2$ resulted in the agglomeration of nanoparticles on the membrane surface as evidenced from SEM study. Additionally, a drop-in porosity value as presented in Table 1 for the M-3.0 membrane compared to the M-2.0 membrane leads to flux depletion. The durability test was conducted over a period of 200 h for the neat PP and M-2.0 membranes at 80 °C. For M-0 membrane, the permeate flux and TDS of the permeate was depleted to 15.6 kg/m^{2}h and 530 ppm, respectively indicating the wetting of the membrane pores by the penetration of water molecules. Whereas, M-2.0 membrane showed an almost stable flux of 43.8 kg/m^{2}h with a permeate TDS of 161 ppm at the end of the experiment representing a superior anti-wetting property.

4. Conclusions

This study demonstrated a facile molecular self-assembly approach for the coating of hydrophobic $HTiO_2$ nanoparticles layer over the microporous PP membrane. The newly synthesized neat PP membrane was porous and a further improvement in porosity with a reduction in pore size was achieved for the coated PP membranes. The high porosity for the coated membranes ascribed to the potentiality of self-assembled TMA layer to generate porous structures on the membrane surface. The PP membranes modified coating were hydrophobic due to the hydrophobic functional groups present on the $HTiO_2$ ensuring a better dispersion in the self-assembled layer. While the decrease in pore size is due to the partial filling of the pores of the PP membrane by the self-assembled TMC network comprised of $HTiO_2$. The LEP gradually increased by the addition of $HTiO_2$ due to the more accumulation of hydrophobic $HTiO_2$ on the membrane surface. The loading of $HTiO_2$ witnessed a slight increase in the surface roughness for the modified PP membrane credited to the least agglomeration of $HTiO_2$. The water flux of modified membranes was increased up to the loading of 2.0wt% $HTiO_2$ with a minor reduction in salt rejection. The less flux for neat PP membranes could be due to the easy trapping of water molecules into the membrane pores, whereas the loading of hydrophobic $HTiO_2$ particles improved pore-wetting resistance with improved flux values. This study confirmed the optimum loading composition of $HTiO_2$ as 2.0 wt%, corresponding to a high flux of 45.4 kg/m^{2}h with the highest durability for the membrane.

Table 3

Water analysis data of Arabian Gulf seawater feed and permeate obtained for M-0 and M-2.0 membranes at 80 °C.

Parameter	Unit	Seawater feed	Permeate (M-0)	Permeate (M-2.0)
pH	-	7.4	7.1	7.1
Conductivity	mS/cm	55.4	0.30	0.29
TDS	ppm	35,854	184	144
Calcium	mg/L	826	13.4	8.16
Magnesium	mg/L	1154	8.1	7.23
Sulfate	mg/L	3600	46	32
Chloride	mg/L	26000	36	31
Sodium	mg/L	14,800	93	86
Boron	mg/L	2.76	0.22	0.16
Nitrate	mg/L	3.6	0.85	0.71
Silica	mg/L	18.2	0.83	0.65
Fluoride	mg/L	4.3	0.17	0.13

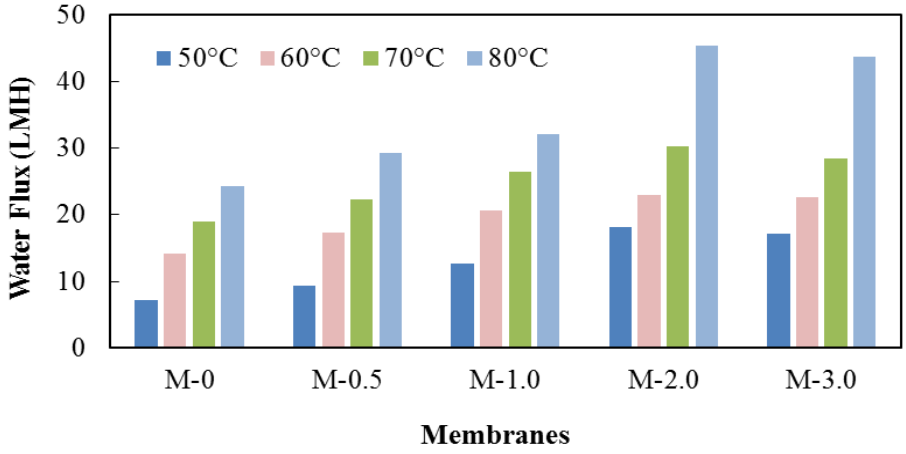

Fig. 6. The water flux of membranes at different temperatures.

Acknowledgement

Authors are thankful to the Kuwait Foundation for Advancement of Sciences for partly funding this project and Kuwait Institute for Scientific Research (KISR) for financially supporting this research activity.

References

[1] A. Alkhudhiri, N. Darwish, N. Hilal, Membrane distillation: A comprehensive review, 287 (2012) 2–18.

[2] E. Drioli, A. Ali, F. Macedonio, Membrane distillation: Recent developments and perspectives, Desalination 356 (2015) 56–84.

[3] D. Behera, A.K. Banthia, Bisgma/Tio_2 organic-inorganic hybrid nanocomposite. Polymer-plastics Tech. Engg. 26 (2007) 10–12.

[4] J.K. Holt, H.G. Park, Y.M. Wang, M. Stadermann, A.B. Artyukhin, C. Grigoropoulos, C.P. Noy, A. Bakajin, Fast mass transport through sub-2-nanometer carbon nanotube, Science 312 (2006) 1034–1037.

[5] P. Rittigstein, R.D. Priestley, L.J. Broadbelt, J.M. Torkelson, Model polymer nanocomposites with known interlayer spacing provide understanding of confinement effects in real nanocomposites, Nature Mat. 6 (2007) 278–282.

[6] Z. Cui, E. Drioli, Y.M. Lee, Recent progress in fluoropolymers for membranes, Prog. Polym. Sci. 39 (2014) 164–198.

[7] L. Yan, K. Wang, L. Ye, Super hydrophobic property of PVDF/$CaCO_3$ nanocomposite coatings, J. Mater. Sci. Lett. 22 **(**2003) 1713–1717.

[8] A. Gugliuzza, E. Drioli. PVDF and HYFLON AD membranes: Ideal interfaces for contactor applications. J. Membr. Sci. 300 **(**2007) 51–62.

[9] N.F. Himma, A.K. Wardani, I.G. Wenten, Preparation of superhydrophobic polypropylene membrane using dip-coating method: the effects of solution and process parameters, Polym. Plastics Technol. Engg. 56 (2017) 184–194.

[10] S.S. Zhou, Z.S. Guan, Y. Pang, Fabrication of polypropylene super-hydrophobic surface using ptfe-coated-sieves template via templating and splitting process, Polym. Plastics Technol. Engg. 51 (2012) 845–848

[11] S. Roy, M. Bhadra, S. Mitra, Enhanced desalination via functionalized carbon nanotube immobilized membrane in direct contact membrane distillation, Sep. Purif. Technol. 136 (2014) 58–65.

[12] Z. Xu, Z. Liu, P. Song, C. Xiao, Fabrication of super-hydrophobic polypropylene hollow fiber membrane and its application in membrane distillation, Desalination 414 (2017) 10–17.

[13] Y. Shao, M. Han,Y. Wang, G. Li, W. Xiao, X. Li, X. Wu, X. Ruan, X. Yan, G. He, X. Jiang, Superhydrophobic polypropylene membrane with fabricated antifouling interface for vacuum membrane distillation treating high concentration sodium/magnesium saline water, J. Membr. Sci. 579 (2019) 240–252.

[14] G.F.L. Xu Dong Sun, Yu Zhong Zhang, Yu Xiang Li, Hong Li, Preparation of super-hydrophobic polyethersulphone membrane by sol–gel method, Adv. Mater. Res. 79–82 (2009) 839–842.

[15] C. Yao, G.S. Gao, X.P. Lin, X.J. Yang, L.D. Lu, X. Wang, Surface modification of nanosized TiO2 with silane coupling reagent, J. Inorg. Mat. 21 (2006) 315–321.

[16] R. Amir, A. Ellen, D. Guangxi, M. Jaleh, C. Vicki, Superhydrophobic modification of TiO_2 nanocomposite PVDF membranes for applications in membrane distillation, J. Membr. Sci. 415–416 (2012) 850–863.

[17] C. Queffelec, M. Petit, P. Janvier, D.A. Knight, B. Bujoli, Surface modification using phosphonic acids and esters, Chem. Rev. 112 (2012) 3777–3807.

[18] A. Mahapatro, T.D.M. Negrón, A. Nguyen, Spectroscopic evaluations of interfacial oxidative stability of phosphonic nanocoatings on magnesium, J. Spectrosc. 2015, Article ID 350630.

[19] R. Quiñones, K. Rodriguez, R.J. Iuliucci, Investigation of phosphonic acid surface modifications on zinc oxide nanoparticles under ambient conditions, Thin Sol. Films 565 (2014) 155–164.

[20] A. Raman, R. Quiñones, L. Barriger, R. Eastman, A. Parsi, E.S. Gawalt, Understanding organic film behavior on alloy and metal oxides, Langmuir 26 (2010) 1747–1754.

[21] S. Szillies, P. Thissen, D. Tabatabai, F. Feil, W. Fürbeth, N. Fink, G. Grundmeier, Formation and stability of organic acid monolayers on magnesium alloy AZ31: The role of alkyl chain length and head group chemistry, Appl. Surf. Sci. 283 (2013) 339–347.

[22] B. Annika, K. Guido, Long Alkyl chain organophosphorus coupling agents for in situ surface functionalization by reactive milling, Inorganics 2 (2014) 410–423.

[23] R. Quiñones, S. Garretson, G. Behnke, J.W. Fagan, K.T. Mueller, S. Agarwal, R.K. Gupta, Fabrication of phosphonic acid films on nitinol nanoparticles by dynamic covalent assembly, Thin Sol. Films, 642 (2017) 195–206.

[24] R. Quiñones, E.S. Gawalt, Study of the formation of self-assembled monolayers on nitinol, Langmuir 23 (2007) 10123–10130.

[25] N. Nakayama, T. Hayashi, Preparation of TiO_2 nanoparticles surface-modified by both carboxylic acid and amine: Dispersibility and stabilization in organic solvents, Colloid surface A 317 (2008) 543-550.

[26] C. Pilar, H. Kian, A. Saffar, A. Abdellah, B.M. Antonio, A. David, Polypropylene-based porous membranes: influence of polymer composition, extrusion draw ratio and uniaxial strain, Polymers 10 (2018) 33.

[27] K. Rajesha, A. Mansour, O. Salim, B. Garudachari, P.T. Jibu. Boron selective thin film composite nanofiltration membrane fabricated via a self-assembled trimesic acid layer at a liquid–liquid interface on an ultrafiltration support, New J. Chem. 43 (2019) 3874–3883.

[28] Y. Yang, D. Rana, T. Matsuura, S. Zheng, C.Q. Lan, Criteria for the selection of a support material to fabricate coated membranes for a life support device, RSC Adv. 4 (2014) 38711–38717.

[29] S. Zhao, Z. Wang, J. Wang, S. Wang, Poly (ether sulfone)/polyaniline nanocomposite membranes: effect of nanofiber size on membrane morphology and properties, Ind. Eng. Chem. Res. 53 (2014) 11468–11477.

[30] T.L.S. Silva, S. Morales-Torres, J.S. Figueiredo, A.M.T. Silva, Multi walled carbon nanotube/PVDF blended membranes with sponge- and finger-like pores for direct contact membrane distillation, Desalination 357 (2015) 233–245.

[31] K. Rajesha, A. Mansour, B. Garudachari, M. Abbas, P.T. Jibu P. Thomas, Hydrophobically modified silica blend PVDF nanocomposite membranes for seawater desalination via direct contact membrane distillation, Desal. Water Treat. 148 (2019) 20–29.

[32] M.M. Ba-Abbad, A.A.H. Kadhum, A.B. Mohamad, M.S. Takriff, K. Sopian, Synthesis and catalytic activity of TiO_2 nanoparticles for photochemical oxidation of concentrated chlorophenols under direct solar radiation, Int. J. Electrochem. Sci. 7 (2012) 4871–4888.

[33] L. Regina, S. Gotthard, J. Evelin, P.A. Hans-Ju¨rgen, Infrared spectra of alkylphosphonic acid bound to Aluminum surfaces, Macromol. Symp. 254 (2007) 248–253.

[34] T. Rachel, O. Rudolf, F. Alex, M. Morteza, M. Mainak, Capillary-force-assisted self-assembly (CAS) of highly ordered and anisotropic graphene-based thin films, J. Phys. Chem. C 118 (2014) 259−267.

[35] M. Lackinger, S. Griessl, W. M. Heckl, M. Hietschold and G. W. Flynn, Self-assembly of trimesic acid at the liquid-solid interface-a study of solvent-induced polymorphism, Langmuir, 21 (2005) 4984−4988.

[36] Y. Ye, W. Sun, Y. Wang, X. Shao, X. Xu, F. Cheng, J. Li and K. Wu, A unified model: self-assembly of trimesic acid on gold, *J. Phys. Chem. C*, 111 (2007) 10138−10141.

[37] H. Zou, S. Wu, J. Shen, Polymer/silica nanocomposites: preparation, characterization, properties, and applications, Chem. Rev. 108 (2008) 3893−3957.

[38] M.S. El-Bourawi, A framework for better understanding membrane distillation separation process, J. Membr. Sci. 285 (2006) 4–29.

[39] K. Smolders, A.C.M. Franken, Terminology for membrane distillation, Desalination, 72 (1989) 249–262.

[40] Pelin Yazgan-Birgia, Mohamed I. Hassan Alib, Hassan A. Arafat, Estimation of liquid entry pressure in hydrophobic membranes using CFD tools, Journal of Membrane Science 552 (2018) 68–76

[41] P.Z. Vladimir, Nanoparticles in a nanochannel: Van der Waals interaction and diffusion, Physics Letters A, 381 (2017) 2832–2836.

[42] N.G. Chloe, H.G. Jessica, P. Nicholas, H. Samir, W.F. Richard, M.B. Serena, E.C. Ruth, Crosslinking and composition influence the surface properties, mechanical stiffness and cell reactivity of collagen-based films, Acta Biomat. 8 (2012) 3080–3090.

[43] G.K. Ayse, S.M. S. Cristina, G. Menemse, M. Giovanni, Surface characteristics of ionically crosslinked chitosan membranes, 106 (2007) 3884–3888.

[44] L.D. Tijing, Y.C. Woo, W.G. Shim, T. He, J.S. Choi, S.H. Kim, H.K. Shon, Superhydrophobic nanofiber membrane containing carbon nanotubes for highperformance direct contact membrane distillation, J. Membr. Sci. 502 (2016) 158–170.

[45] Y. Liao, R. Wang, A.G. Fane, Fabrication of bioinspired composite nanofiber membranes with robust superhydrophobicity for direct contact membrane distillation, Environ. Sci. Technol. 48 (2014) 6335–6341.

[46] C.L. Su, J.J. Chang, K.X. Tang, F. Gao, Y.P. Li, H.B. Cao, Novel three-dimensional superhydrophobic and strength-enhanced electrospun membranes for long-term membrane distillation, Sep. Purif. Technol. 178 (2017)279–287.

[47] Y. Kang-Kang, J. Lei, L. Saisai, J. Xiaosheng, L. Yin, Z. Lin, Superhydrophobic electrospun nanofiber membrane coated by carbon nanotubes network for membrane distillation, Desalination 437 (2018) 26–33.

[48] Y. Liao, R. Wang, A.G. Fane, Fabrication of bioinspired composite nanofiber membranes with robust superhydrophobicity for direct contact membrane distillation, Environ. Sci. Technol. 48 (2014) 6335–6341.

[49] C.L. Su, J.J. Chang, K.X. Tang, F. Gao, Y.P. Li, H.B. Cao, Novel three-dimensional superhydrophobic and strength-enhanced electrospun membranes for long-term membrane distillation, Sep. Purif. Technol. 178 (2017) 279–287.